EXPLORING THE HIGH-ENERGY NEUTRINO UNIVERSE FROM THE SOUTH POLE – RESULTS FROM AMANDA AND STATUS OF ICECUBE

Kurt Woschnagg

Dept. of Physics, University of California, Berkeley, CA 94720, USA

for the AMANDA collaboration [?]

Abstract

The Antarctic Muon And Neutrino Detector Array (AMANDA) is a neutrino telescope embedded deep in the 2.8 km-thick polar icecap at the South Pole. AMANDA aims to detect high-energy cosmic neutrinos from sources where the highest-energy cosmic rays are produced and accelerated. We present recent results from AMANDA on searches for high-energy neutrinos of extraterrestrial origin. We have searched for a diffuse flux of neutrinos, neutrino point sources, and neutrinos from GRBs and from WIMP annihilations in the Sun or the center of the Earth. We also present a preliminary result on the first energy spectrum above a few TeV for atmospheric neutrinos. The status of IceCube, the km^3-sized successor to AMANDA, is reviewed after its first successful construction season.

1   Introduction

In observational astronomy and astrophysics, the properties of cosmological objects are studied through the detection of cosmic information carriers emitted by the objects. Three types of messengers have been used to date: electromagnetic radiation (photons), cosmic rays, and neutrinos (figure **??**).
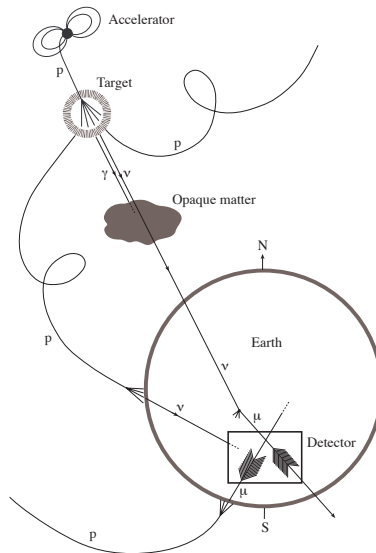

Figure 1: *High-energy astrophysical information carriers: cosmic rays (p) are deflected by magnetic fields; photons (γ) are absorbed by intervening matter; neutrinos (ν) point back to their source and can traverse great distances. For neutrino detection, Earth is used as a filter against cosmic rays.*

The electrically neutral photons are not deflected by intergalactic magnetic fields and therefore point back to their origin, but are absorbed by intervening matter and interactions with the microwave and infrared backgrounds. Furthermore, photons cannot yield any information on the internal processes of the sources since they are produced in their outer regions. Cosmic rays, composed of nuclei, are deflected by magnetic fields, and suffer energy losses during propagation which deforms their energy spectrum. Neutrinos, which

have no electric charge and a low interaction cross-section with matter, can travel cosmological distances un-deflected by magnetic fields, and the distance at which the Universe can be observed is limited only by the strength of the source. They can thus retain the complete source flux and spectral information when reaching the Earth. On the other hand, due to the low interaction cross-section, neutrino detection requires very large detector volumes and long exposure times.

The existence of high-energy cosmic neutrinos is suggested by the observation of high-energy cosmic rays and gamma rays. Observation of cosmic neutrinos could shed light on the production and acceleration mechanisms of cosmic rays, which are not understood for energies above the "knee" at 10^{15} eV. Neutrinos with energies in the TeV range and higher may be produced by a variety of sources. Candidate cosmic accelerators include supernova remnants, the accretion disk and jets of Active Galactic Nuclei (AGN), and the violent processes behind Gamma Ray Bursts (GRB). In these environments, neutrinos are expected to be produced in the decays of pions created through proton-proton or proton-photon collisions. The expected neutrino energy spectrum from such accelerators is typically predicted to be E^{-2}. The AMANDA detector was built to explore the high-energy universe in neutrinos, using the advantages of neutrinos as cosmic messengers. In January 2005, construction began on IceCube [?], the km^3-sized successor to AMANDA.

2   The AMANDA Neutrino Telescope

The AMANDA detector [?] consists of 677 optical modules arranged along 19 vertical strings buried deep in the glacial ice at the South Pole, mainly at depths between 1500 and 2000 m (figure **??**). Each module consists of a photomultiplier tube (PMT) housed in a spherical glass pressure vessel. PMT pulses are transmitted to the data acquisition electronics at the surface via coaxial cables (inner 4 strings), twisted pair cables (6 strings) or optical fibers (outer 9 strings). The geometric outline of the bulk of the array is a cylinder which is 500 m high and with a radius of 100 m. The typical vertical spacing between modules is 10–20 m, and the horizontal spacing between strings 30–50 m.

The optical modules record Cherenkov light generated by secondary charged leptons (e, μ, τ) created in neutrino interactions near the detector. Events are
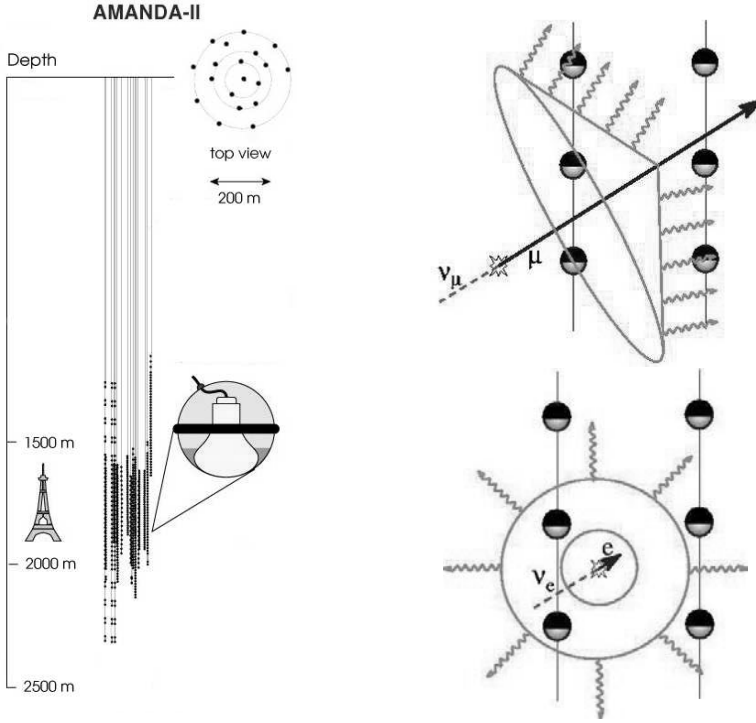
Figure 2: *Schematic view of the AMANDA neutrino telescope and event signatures for ν_μ-induced muon tracks and ν_e-induced cascades.*

reconstructed **?)** by maximizing the likelihood that the timing pattern of the recorded light is produced by a hypothetical track or cascade[1] (see figure **??**). The angular resolution is between 1.5° and 2.5° for muon tracks, depending on declination, and ~30° for cascades, the difference reflecting the fact that muon tracks yield a long lever arm whereas cascades produce more spherical light patterns. On the other hand, the energy resolution, which is correlated to the amount of detected light, is better for cascades, 0.15 in $\log(E)$, than for muon tracks, 0.4 in $\log(E)$.

Using calibration light sources deployed with the strings and a YAG laser

---

[1]A cascade is an electromagnetic or hadronic shower.

at the surface connected to diffusing balls in the ice via optical fibers, we have mapped [?] the optical properties of the ice over the full relevant wavelength- and depth range (figure ??). The glacial ice is extremely transparent for Cherenkov wavelengths near the peak sensitivity of the modules: at 400 nm, the average absorption length is 110 m and the average effective scattering length is 20 m. Below a depth of 1500 m, both scattering and absorption are dominated by dust, and the optical properties vary with dust concentration. The depth profile is in good agreement with variations of dust concentration measured in ice cores from other Antarctic sites [?, ?, ?]. These dust layers reflect past variations in climate. Implementation of the detailed knowledge of ice properties into our detector simulation and reconstruction tools reduces systematic uncertainties and improves track and cascade reconstruction.
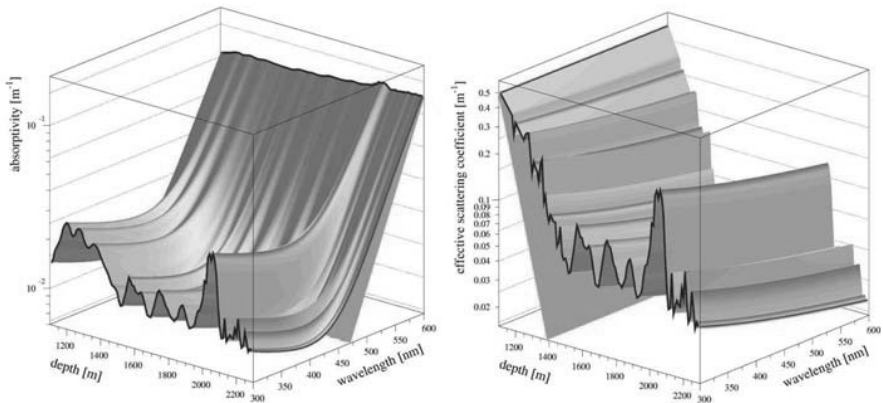

Figure 3: *Optical properties of deep South Pole ice: absorptivity (left) and scattering coefficient (right) as function of depth and wavelength. The green (partially obscured) tilted planes show the contribution from pure ice to absorption and from air bubbles to scattering, respectively. If these contributions are subtracted, the optical properties vary with the concentration of insoluble dust, which tracks climatological variations in the past* [?, ?, ?].

The full 19-string array, named AMANDA-II, started taking data in 2000. An earlier 10-string stage (comprising the inner 10 strings), called AMANDA-B10, took data in the period 1997–1999. In the 2003/04 field season, the data

acquisition system was upgraded with Transient Waveform Recorders on all channels, digitizing the PMT pulses in the electronics on the surface. Waveform digitization will increase the effective dynamic range of individual channels by about a factor 100 and will lead to an improvement in energy reconstruction, especially at high energies.

3 Physics Topics and Analysis Strategies

AMANDA is used to explore a variety of physics topics, ranging from astrophysics to particle physics, over a wide range of energies. At the low energy end, in the MeV range, AMANDA is sensitive to bursts of antineutrinos from supernovae (which would be detected by a collective rate increase in all PMTs). For higher energies, GeV to TeV, the detector is used to study atmospheric neutrinos and to conduct indirect dark matter searches. In the energy range for which AMANDA has been primarily optimized, TeV to PeV, the aim is to use neutrinos to study AGN and GRBs, looking both for a diffuse flux and for point sources of high-energy neutrinos. Using special analysis techniques, the array is also sensitive to the ultra-high energies in the PeV to EeV range.

For most analysis channels, AMANDA uses the Earth as a filter and looks down for up-going neutrinos. The main classes of background are up-going atmospheric neutrinos and down-going atmospheric muons that are misreconstructed as up-going. Since AMANDA is located at the South Pole, an up-going event will have originated in the Northern sky.

We present all flux limits following the ordering scheme by Feldman and Cousins [?] and include systematic uncertainties in the limit calculations according to the method derived by Conrad *et al.* [?] The main sources of systematic uncertainty in the analyses presented here are the modelling of muon propagation and of optical ice properties in the detector simulation, adding up to roughly 25% uncertainty.

The AMANDA collaboration adheres strictly to a policy of performing all analyses in a "blind" manner to ensure statistical purity of the results. In practice, this means that selection criteria are optimized either on a sub-sample of the data set which is then excluded from the analysis yielding the final result, or on a time-scrambled data set which is only unscrambled after the selection criteria have been optimized and finalized.

4   Atmospheric Neutrinos

Neutrinos, and to some extent muons, created by cosmic ray interactions in the atmosphere constitute the main background in most analysis channels (the atmospheric muon flux is five orders of magnitude larger than the expected neutrino flux), but also serve as a test beam with which to study the detector response. Since the overwhelming majority of up-going neutrinos detected by AMANDA, even in the presence of a signal from an extraterrestrial source, are generated in the atmosphere by cosmic rays, we can study atmospheric neutrinos with high statistics at energies that have been out of reach for other neutrino detectors. Using a neural net energy reconstruction, trained on a full detector and physics simulation, followed by regularized unfolding, we measure a preliminary energy spectrum for up-going neutrinos with year 2000 AMANDA-II data (figure **??**). This is the first atmospheric neutrino spectrum above a few
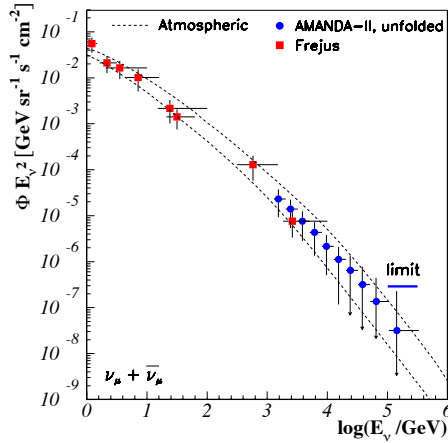

Figure 4: *Atmospheric neutrino energy spectrum (preliminary) from regularized unfolding of AMANDA data, compared to the Fréjus spectrum* **?)** *at lower energies. The two dashed curves are model predictions (based on separate parametrizations below* **?)** *and above* **?)** *100 GeV) for the horizontal (upper) and vertical (lower) flux. The thick solid horizontal line indicates the limit we derive (section* **??**) *on an E^{-2} flux of extraterrestrial muon neutrinos.*

TeV, and it extends up to 300 TeV. It is in good agreement with theoretical predictions and smoothly extends the spectrum measured at lower energies by Fréjus [?].

5   Searches for a Diffuse Flux of Cosmic Neutrinos

The ultimate goal of AMANDA is to find and study the properties of cosmic sources of high-energy neutrinos. Should individual sources be too weak to produce an unambiguous directional signal in the array, the integrated neutrino flux from all sources could still produce a detectable diffuse signal. We have searched several years of data for such a diffuse signal using complementary techniques in different energy regimes.

5.1   Atmospheric neutrino spectrum

The atmospheric neutrino spectrum (fig. **??**) was used to set a preliminary upper limit on a diffuse E^{-2} flux of extraterrestrial muon neutrinos for the energy range covered by the highest bin, 100–300 TeV, by calculating the maximal non-atmospheric contribution to the flux in the bin given its statistical uncertainty. However, the bins in the unfolded spectrum are correlated and the uncertainty in the last bin can not a priori be assumed to be Poissonian. The statistics in the bin were therefore determined with a Monte Carlo technique used to construct confidence belts following the definition by Feldman and Cousins [?]. Given the unfolded number of experimental events in the bin (a fractional number), a preliminary 90% C.L. upper limit of

$$E^2 \Phi_{\nu_\mu}(E) < 2.6 \times 10^{-7} \text{ GeV cm}^{-2} \text{ s}^{-1} \text{ sr}^{-1} \tag{1}$$

was derived for 100 TeV $< E_\nu <$ 300 TeV, which includes 33% systematic uncertainties.

5.2   Cascades

In the cascade channel, AMANDA has essentially 4π coverage, and is sensitive to all three neutrino flavors. The year 2000 data sample, corresponding to 197 days livetime, was searched for cascade events. Event selection was based on topology and energy, and optimized to maximize the sensitivity to an E^{-2} signal spectrum. After final cuts one event remains, with an expected background

of $0.90^{+0.69}_{-0.43}$ from atmospheric muons and $0.06^{+0.09}_{-0.04}$ from atmospheric neutrinos. Not having observed an excess over background, we calculate a limit on a signal flux. The 90% C.L. limit on a diffuse flux of neutrinos of all flavors for neutrino energies between 50 TeV and 5 PeV, assuming full flavor mixing so that the neutrino flavor ratios are 1:1:1 at the detector, is

$$E^2\Phi_\nu(E) < 8.6 \times 10^{-7} \text{ GeV cm}^{-2}\text{ s}^{-1}\text{ sr}^{-1}. \tag{2}$$

Since the energy range for this analysis contains the energy of the Glashow resonance, a limit on the flux at 6.3 PeV can be derived:

$$E^2\Phi_{\bar{\nu}_e}(6.3\,\text{PeV}) < 2 \times 10^{-6} \text{ GeV cm}^{-2}\text{ s}^{-1}\text{ sr}^{-1}. \tag{3}$$

These limits [?] obtained with one year (2000) of AMANDA-II data are roughly a factor 10 lower than the limits from similar searches performed with AMANDA-B10 data from 1997 [?] and 1999 [?].

5.3 Ultra High Energy neutrinos

At ultra-high energies (UHE), above 1 PeV, the Earth is opaque to electron- and muon-neutrinos. Tau neutrinos with such initial energies might penetrate the Earth through regeneration [?], in which the τ produced in a charged-current ν_τ interaction decays back into ν_τ, but they will emerge with much lower energies. The search for extraterrestrial UHE neutrinos is therefore concentrated on events close to the horizon and even from above. The latter is possible since the atmospheric muon background is low at these high energies due to the steeply falling spectrum. Our search for UHE events in 1997 AMANDA-B10 data (131 days of livetime) relies on parameters that are sensitive to the expected characteristics of an UHE signal: bright events, long tracks (for muons), low fraction of single photoelectron hits. A neural net was trained to optimize the sensitivity to an E^{-2} neutrino signal in data dominated by atmospheric neutrino background.

After final selection, 5 data events remain, with 4.6 ($\pm 36\%$) expected background. Thus, no excess above background is observed and we derive [?] a 90% C.L. limit on an E^{-2} flux of neutrinos of all flavors, assuming a 1:1:1 flavor ratio at Earth, for energies between 1 PeV and 3 EeV, of

$$E^2\Phi_\nu(E) < 0.99 \times 10^{-6} \text{ GeV cm}^{-2}\text{ s}^{-1}\text{ sr}^{-1}. \tag{4}$$

A similar analysis of AMANDA-II data from 2000 is under way. However, the bright UHE events also saturate the larger array, so a substantial gain in sensitivity will mainly be due to the additional exposure time and improved selection algorithms.

5.4   Summary of diffuse searches

Using different analysis techniques, AMANDA has set limits on the diffuse flux of neutrinos with extraterrestrial origin for neutrino energies from 6 TeV [?] up to a few EeV (figure ??). With the exception of the limit from the unfolded atmospheric spectrum, which can be seen as a quasi-differential limit, the limits are on the integrated flux over the energy range which contains 90% of the signal. Our limits exclude, at 90% C.L., some models [?, ?] predicting diffuse neutrino fluxes.
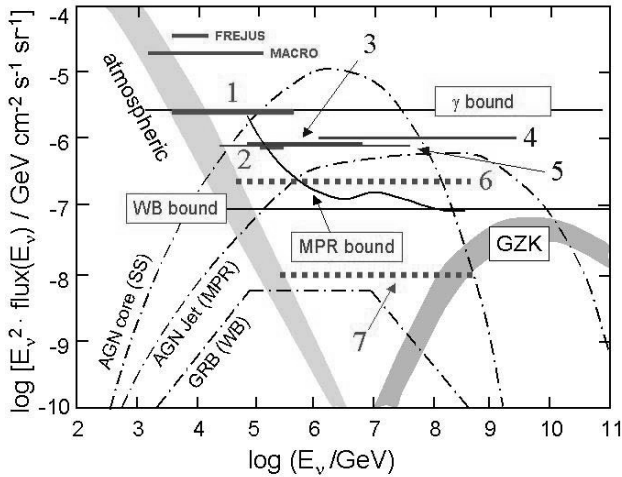

Figure 5: *Limits on a diffuse flux of neutrinos of all flavors with an E^{-2} energy spectrum: (1) from ν_μ in 1997 AMANDA-B10 data; (2) from unfolded 2000 atmospheric neutrino spectrum; (3) from 2000 cascades; (4) from 1997 UHE events; (5) Baikal cascades 1998-2003; (6) sensitivity for 4 years of AMANDA data; (7) sensitivity for 3 years of IceCube data.*

6   Point Source Searches

Searches for neutrino point sources require good pointing resolution and are thus restricted to the ν_μ channel. We have searched AMANDA-II data from 2000–2003 (corresponding to 807 days of livetime) for a point source signal. Events were selected to maximize the model rejection potential [?)] for a hypothetical E^{-2} neutrino spectrum convoluted with the background spectra due to atmospheric neutrinos and misreconstructed atmospheric muons. The selection criteria were optimized for the combined 4-year data set in each declination band separately since the geometry of the detector array introduces declination-dependent efficiencies. The *sensitivity* of the analysis, defined as the average upper limit one would expect to set on a non-atmospheric neutrino flux if no signal is detected, is shown in figure **??** for an E^{-2} signal spectrum.
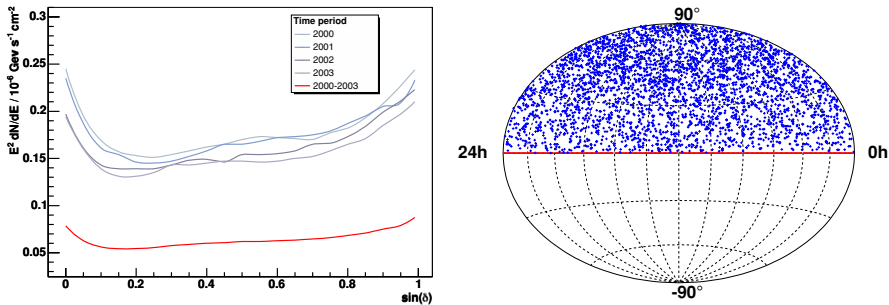

Figure 6: *Left*: *Sensitivity for an E^{-2} flux spectrum as function of declination.* Right*: Sky plot for 3329 up-going neutrino candidates in 4-year data sample.*

The final sample (figure **??**, right) of 3329 neutrino candidates below the horizon, i.e. from the Northern sky, (with 3438 expected atmospheric neutrinos) was scanned for point sources with two methods. In the first, the sky is divided into a (repeatedly shifted) fine-meshed grid of overlapping bins which are tested for a statistically significant excess over the background expectation (estimated from all other bins in the same declination band). This search yielded no evidence for extraterrestrial point sources. The second method is an unbinned

search, in which the sky locations of the events and their uncertainties from reconstruction are used to construct a sky map of *significance* in terms of fluctuation (in σ) over background (figure **??**). This map displays only one potential hot spot (above 3σ) with $\sigma = 3.4$, which is well within the expectation from a random event distribution. For comparison, similar significance maps were constructed after randomizing the right ascension for all events, thus simulating a truly random distribution (one such map is shown in the middle panel of figure **??**). These scrambled maps are statistically indistinguishable from the real (upper) map. A full statistical analysis of many such scrambled maps proves that the sky map is fully compatible with a distribution expected from an atmospheric neutrino sample. The bottom panel in figure **??** shows the distribution of the highest significance found in 1000 scrambled maps. The probability for finding $\sigma_{max} = 3.4$ or higher in a random map is 92%. We thus see no evidence for point sources with an E^{-2} energy spectrum based on the first four years of AMANDA-II data. This preliminary result complements previously published results from point source searches with the AMANDA-B10 detector [?] and the first year [?] and first three years [?] of AMANDA-II data. Adding two more years of data to the one-year sample increased the sensitivity by a factor of 2.2.

7   Search for Neutrinos from GRBs

A special case of point source analysis is the search for neutrinos coincident with gamma ray bursts (GRBs) detected by satellite-borne detectors. For this search, the timing of the neutrino event serves as an additional selection handle which significantly reduces background. We have used samples of GRBs observed by two gamma ray detector systems: the BATSE instrument on board the CGRO satellite, which was decommissioned in 2000, and the Third Interplanetary Network (IPN3), a group of spacecraft equipped with gamma-ray burst detectors which uses triangulation to spatially locate the bursts.

For each burst, AMANDA data in a 10 min window around the GRB time (here defined as the start of T_{90}, the period which covers 90% of the γ-ray signal) was kept blind. The background was estimated by averaging over events in the on-source spatial bin within ± 1 hour of the burst (excluding the 10 min signal window). Data was then searched for a statistically significant excess over background within T_{90} (which is contained within the blind window).
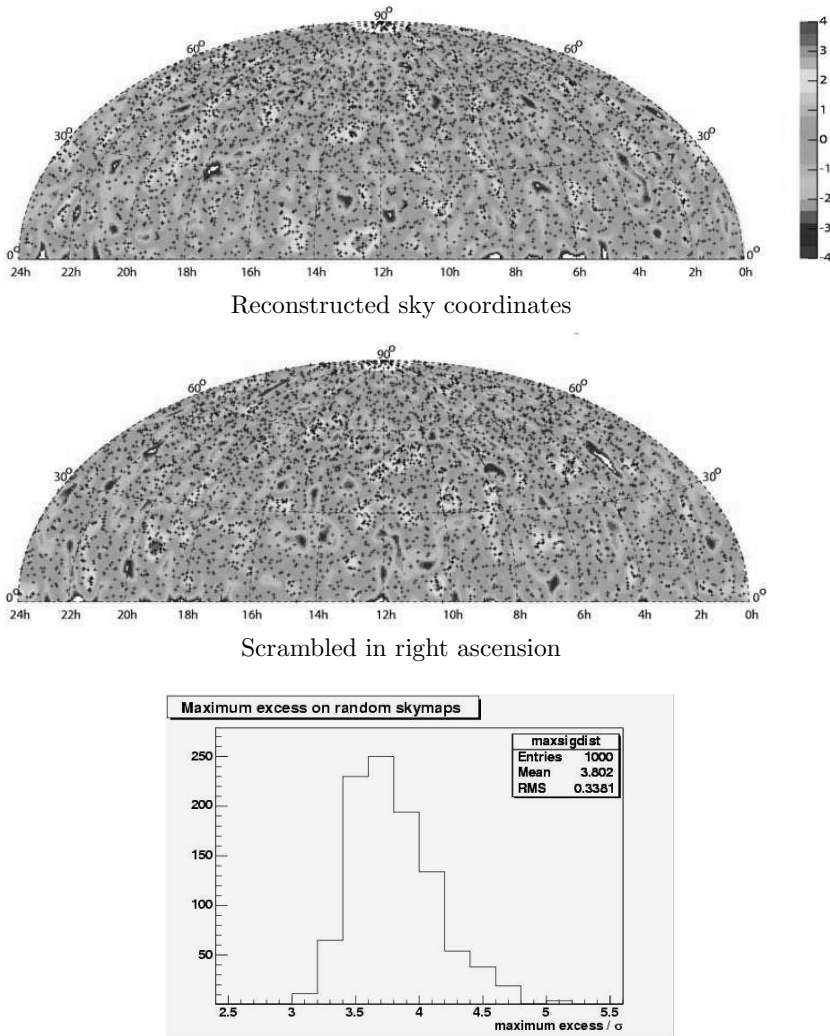
Figure 7: *Significance map (top) constructed from 3329 up-going events in the final sample from a point source search with AMANDA-II data from 2000–2003. The points show the reconstructed sky positions (declination and right ascension) of the neutrino candidates. The color scale indicates the significance (in σ). The highest significance is σ = 3.4. The middle panel shows an example of a significance map based on the same events, but with randomized right ascension coordinates. The bottom panel shows the distribution of highest significance from 1000 scrambled sky maps.*

We have initially analyzed a sample of only BATSE-triggered bursts. We found no neutrino event coincident with any of 312 bursts recorded between 1997, when AMANDA-B10 became operational, and 2000, when BATSE operations ended, and derived a preliminary limit on the muon neutrino flux [?]. Recently, we have performed a similar search on a sample containing 139 bursts triggered by BATSE and/or IPN between 2000 and 2003. As in the previous analysis, no neutrino event was observed in coincidence with any of the bursts, in this case with an average of 1.25 expected from background fluctuations. Assuming a broken power-law energy spectrum as proposed by Waxmann and Bahcall [?], with $E_{\text{break}} = 100$ TeV and $\Gamma_{\text{bulk}} = 300$, we obtain a (preliminary) 90% C.L. upper limit on the expected muon neutrino flux at the Earth of

$$E^2 \Phi_\nu(E) < 3 \times 10^{-8} \text{ GeV cm}^{-2} \text{ s}^{-1} \text{ sr}^{-1} \qquad (5)$$

based on the 139 burst sample.

We are currently expanding our GRB-neutrino searches to include cascade events. In the cascade analysis, the 4π coverage together with the temporal coincidence requirement compensate for the poor pointing resolution. In addition, an analysis modeling the flux of coincident neutrinos, based on the discrete set of electromagnetic parameters associated with individual GRBs, is being performed in the context of the fireball phenomenology [?].

8   Dark Matter Searches

Particle physics provides an interesting candidate for non-baryonic dark matter in the Weakly Interacting Massive Particle (WIMP). In particular, the Minimal Supersymmetric extension of the Standard Model (MSSM) provides a promising WIMP candidate in the neutralino, which could be the lightest supersymmetric particle. Neutralinos can be gravitationally trapped in massive bodies, and can then via annihilation and decay of the resulting particles produce neutrinos. AMANDA can therefore perform indirect dark matter searches by looking for fluxes of neutrinos from the center of the Earth or the Sun.

For the former, we present a preliminary update to our published limits obtained with one year of 10-string data [?]. We have looked for vertically up-going tracks in AMANDA-B10 data from 1997 to 1999, corresponding to a total livetime of 422 days. No WIMP signal was found and a 90% C.L. upper
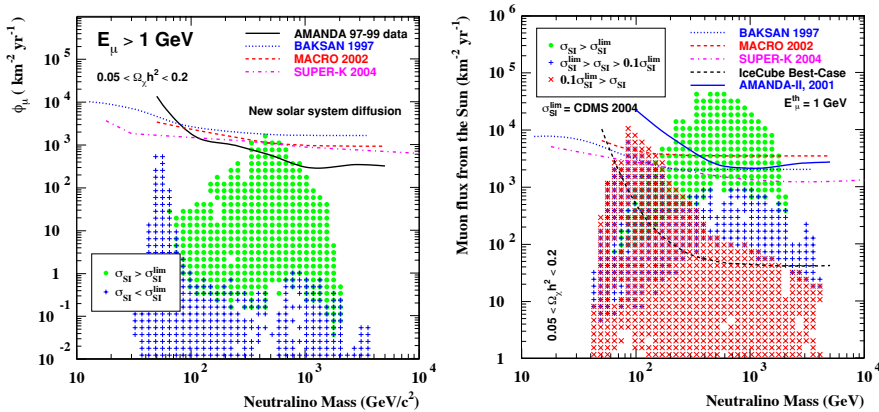
Figure 8: *Preliminary limits on the muon flux due to neutrinos from neutralino annihilations in the center of the Earth (left) and the Sun (right). The colored symbols correspond to model predictions* [?]) *within the allowed parameter space of the MSSM. The green models are disfavored by direct searches with CDMS II* [?]).

limit on the muon flux from the center of the Earth was set for neutralino masses between 50 GeV and 5 TeV (figure ??, left panel).

Due to its larger mass (resulting in a deeper gravitational well) and a higher capture rate due to additional spin-dependent processes, the Sun can also be used for WIMP searches despite its much larger distance from the detector. Although the Sun is maximally 23° below the horizon at the South Pole, AMANDA-II can be used for a WIMP search thanks to its improved reconstruction capabilities for horizontal tracks. Analysis of 2001 data (0.39 years of livetime) yielded no WIMP signal. The preliminary upper limit on the muon flux from the Sun is compared to MSSM predictions [?]) in figure ?? (right panel).

For heavier neutralino masses, the limit obtained with less than one year of AMANDA-II data is already competitive with limits from indirect searches with detectors that have several years of integrated livetime. The green points

in figure **??** correspond to models that are disfavored by direct searches **?)**, which appear to set more severe restrictions on the allowed parameter space than indirect searches. However, it should be noted that the two methods are complementary in that they (a) probe the WIMP distribution in the solar system at different epochs and (b) are sensitive to different parts of the velocity distribution.

9   Status of IceCube

The successful operation of AMANDA has lead to a cubic-kilometer extension to be built in the same location: the IceCube telescope **?)**. This array will comprise 4800 digital optical modules (DOM) on 80 strings, instrumenting one km^3 of ice at depths between 1450 and 2450 m. The modules have digitizing electronics on-board, and only digitial PMT waveform information is sent to the surface. In January 2005, the first string was deployed. All 60 DOMs are operational after refreeze of the hot-water-drilled hole containing the string. Construction will continue until 2010 when the array is expected to be fully commissioned.

References

1. O. Botner *et al.*, Nucl. Phys. B (Proc. Suppl.) **143**, 367 (2005).

2. E. Andrés *et al.*, Nature **410**, 441 (2001).

3. J. Ahrens *et al.*, Nucl. Instrum. Meth. A **524**, 169 (2004).

4. K. Woschnagg *et al.*, in preparation.

5. J. R. Petit *et al.*, Nature **399**, 429 (1999).

6. L. Augustin *et al.*, Nature **429**, 623 (2004).

7. O. Watanabe *et al.*, Ann. Glaciol. **29**, 176 (1999).

8. G. J. Feldman and R. D. Cousins, Phys. Rev. D **57**, 3873 (1998).

9. J. Conrad *et al.*, Phys. Rev. D **67**, 012002 (2003).

10. W. Rhode *et al.*, Astropart. Phys. **4**, 217 (1996).

11. M. Honda *et al.*, Phys. Rev. D **52**, 4985 (1995).

12. L. V. Volkova and G. T. Zatsepin, Sov. J. Nucl. Phys. **37**, 212 (1980).

13. M. Ackermann *et al.*, Astropart. Phys. **22**, 127 (2004).

14. J. Ahrens *et al.*, Phys. Rev. D **67**, 012003 (2003).

15. F. Halzen and D. Saltzberg, Phys. Rev. Lett. **81**, 4305 (1998).

16. M. Ackermann *et al.*, Astropart. Phys. **22**, 339 (2005).

17. J. Ahrens *et al.*, Phys. Rev. Lett. **90**, 251101 (2003).

18. F. W. Stecker and M. H. Salamon, Space Sci. Rev. **75**, 341 (1996).

19. L. Nellen, Phys. Rev. D **47**, 5270 (1993).

20. G. C. Hill and K. Rawlins, Astropart. Phys. **19**, 393 (2003).

21. J. Ahrens *et al.*, Astrophys. J. **583**, 1040 (2003).

22. J. Ahrens *et al.*, Phys. Rev. Lett. **92**, 071102 (2004).

23. M. Ackermann *et al.*, Phys. Rev. D **71**, 077102 (2005).

24. R. Hardtke *et al.*, Proc. 28th Int. Cosmic Ray Conf. (ed. T. Kajita *et al.*, Tsukuba, August 2003), 2717 (University Academy Press, Tokyo, 2003).

25. J. Bahcall and E. Waxmann, Phys. Rev. D **64**, 023002 (2001).

26. M. Stamatikos *et al.*, AIP Conf. Proc. **727**, 146 (2004).

27. D. S. Akerib *et al.*, Phys. Rev. Lett. **93**, 211301 (2004).

28. J. Ahrens *et al.*, Phys. Rev. D **66**, 032006 (2002).

29. J. Edsjö, Nucl. Phys. B (Proc. Suppl.) **143**, 435 (2005).

30. `http://icecube.wisc.edu`

* . The AMANDA collaboration:

M. Ackermann[4], J. Ahrens[11], D. W. Atlee[8], X. Bai[1], R. Bay[9], M. Bartelt[2],
S. W. Barwick[10], T. Becka[11], K.-H. Becker[2], J. K. Becker[7], E. Bernardini[4], D. Bertrand[3],
D. J. Boersma[4], S. Böser[4], O. Botner[17], A. Bouchta[17], O. Bouhali[3], J. Braun[15],
C. Burgess[18], T. Burgess[18], T. Castermans[13], D. Chirkin[6], J. A. Coarasa[8], B. Collin[8],
J. Conrad[17], J. Cooley[15], D. F. Cowen[8], A. Davour[17], C. De Clercq[19], T. DeYoung[12],
P. Desiati[15], P. Ekström[18], T. Feser[11], T. K. Gaisser[1], R. Ganugapati[15], H. Geenen[2],
L. Gerhardt[10], A. Goldschmidt[6], A. Groß[7], A. Hallgren[17], F. Halzen[15], K. Hanson[15],
D. Hardtke[9], R. Hardtke[15], T. Harenberg[2], T. Hauschildt[4], K. Helbing[6], M. Hellwig[11],
P. Herquet[13], G. C. Hill[15], J. Hodges[15], D. Hubert[19], B. Hughey[15], P. O. Hulth[18],
K. Hultqvist[18], S. Hundertmark[18], J. Jacobsen[6], K.-H. Kampert[2], A. Karle[15],
J. Kelley[15], M. Kestel[8], L. Köpke[11], M. Kowalski[4], M. Krasberg[15], K. Kuehn[10],
R. Lang[4], H. Leich[4], M. Leuthold[4], J. Lundberg[17], J. Madsen[16], K. Mandli[15],
P. Marciniewski[17], H. S. Matis[6], C. P. McParland[6], T. Messarius[7], Y. Minaeva[18],
P. Miočinović[9], R. Morse[15], K. Münich[7], R. Nahnhauer[4], J. W. Nam[10], T. Neunhöffer[11],
P. Niessen[1], D. R. Nygren[6], Ph. Olbrechts[19], C. Pérez de los Heros[17], D. Pieloth[4],
A. C. Pohl[5], R. Porrata[9], P. B. Price[9], G. T. Przybylski[6], K. Rawlins[15], E. Resconi[4],
W. Rhode[7], M. Ribordy[13], S. Richter[15], H.-G. Sander[11], K. Schinarakis[2], S. Schlenstedt[4],
D. Schneider[15], R. Schwarz[15], S. H. Seo[8], A. Silvestri[10], M. Solarz[9], G. M. Spiczak[16],
C. Spiering[4], M. Stamatikos[15], D. Steele[15], P. Steffen[4], R. G. Stokstad[6], K.-H. Sulanke[4],
I. Taboada[9], O. Tarasova[4], L. Thollander[18], S. Tilav[1], J. Vandenbroucke[9], L. C. Voicu[8],
B. Voigt[4], W. Wagner[7], C. Walck[18], M. Walter[4], Y. R. Wang[15], C. H. Wiebusch[2],
R. Wischnewski[4], H. Wissing[4], K. Woschnagg[9], G. Yodh[10]

(1) *Bartol Research Institute, University of Delaware, Newark, DE 19716, USA*
(2) *Dept. of Physics, Bergische Universität Wuppertal, D-42097 Wuppertal, Germany*
(3) *Université Libre de Bruxelles, Science Faculty CP230, B-1050 Brussels, Belgium*
(4) *DESY-Zeuthen, D-15735 Zeuthen, Germany*
(5) *Dept. of Technology, Kalmar University, S-39182 Kalmar, Sweden*
(6) *Lawrence Berkeley National Laboratory, Berkeley, CA 94720, USA*
(7) *Institute of Physics, University of Dortmund, D-44221 Dortmund, Germany*
(8) *Dept. of Physics, Pennsylvania State University, University Park, PA 16802, USA*
(9) *Dept. of Physics, University of California, Berkeley, CA 94720, USA*
(10) *Dept. of Physics and Astronomy, University of California, Irvine, CA 92697, USA*
(11) *Institute of Physics, University of Mainz, D-55099 Mainz, Germany*
(12) *Dept. of Physics, University of Maryland, College Park, MD 20742, USA*
(13) *University of Mons-Hainaut, B-7000 Mons, Belgium*
(15) *Dept. of Physics, University of Wisconsin, Madison, WI 53706, USA*
(16) *Physics Dept., University of Wisconsin, River Falls, WI 54022, USA*
(17) *Division of High Energy Physics, Uppsala University, S-75121 Uppsala, Sweden*
(18) *Dept. of Physics, Stockholm University, S-10691 Stockholm, Sweden*
(19) *Vrije Universiteit Brussel, Dienst ELEM, B-1050 Brussels, Belgium*